J Fluoresc (2012) 22:993–1002
DOI 10.1007/s10895-012-1037-1

ORIGINAL PAPER

Dye Doped Eosin Yellowish Silica Nanoparticles as Novel Fluorophore for a Peroxyoxalate Chemiluminescence System

Abdollah Yari · Marzieh Saidikhah

Received: 11 November 2011 / Accepted: 1 January 2012 / Published online: 8 January 2012

Abstract In this work, we report the preparation and characterization of novel dye doped fluorophore Eosin yellowish silica nanoparticles (ESNPs). We synthesized ESNPs by the Stöber method via encapsulation of Eosin Yellowish in silica particles by the condensation of tetraethyl orthosilicate under alkaline condition at room temperature. The resulted ESNPs were characterized by transmission electron microscopy, atomic force microscopy; UV–Visible, fluorescence and Fourier transform infrared spectroscopy. The sizes of the nanoparticles have been found to be 300.0 (±1.0), 400.0 (±1.1) and 500.0 (±5.2) nm depending the reaction conditions under which they were synthesized. Furthermore, because of intense light emission, the ESNPs were used as fluorophore in a peroxyoxalate chemiluminescence system. The effect of solvent and concentrations of necessary reagents, bis(2,4,6-trichlorophenyl)oxalate, sodium salicylate, hydrogen peroxide and the effects of size of the ESNP and temperature on the luminescence efficiency of the system were examined. The activation kinetic parameters of the system were also evaluated from the temperature investigation.

Keywords Chemiluminescence · Doped silica nanoparticles · Eosin yellowish · Peroxyoxalate

Introduction

Dye doped silica (DDS) nanoparticles (NPs) as a new type of fluorophores has been developed in recent years [1–5]. Application of DDS NPs has recently aroused much interest due to their large surface area, high photostability, chemical stability and easy surface modification for bioconjugation [3–8]. Generally, two methods can be used to prepare silica nanoparticles: the Stöber synthesis [9] and the reverse microemulsion method [10]. However, the Stöber method is a robust and easy-to-implement technique, which involves the hydrolysis of tetraethyl orthosilicate (TEOS) in an ethanol solution at room temperature and the reaction is catalyzed by ammonia. The resulting NPs have spherical shapes and narrow size distributions [9, 11].

2′,4′,5′,7′-tetrabromo fluorescein disodium salt or Eosin Yellowish (EY, Fig. 1) is a well-known fluorescent dye and one of the derivatives of fluorescein that has been used as photosensitizer on semiconductors, histological tissue sections and fluorescent labels [12–14]. We believe that one could construct emitting elements by doping EY that be used as useful chemosensors in analytical purposes.

Chemiluminescence is the generation of electromagnetic radiation as light by the release of energy from a chemical reaction that involves the production of an electronically excited species from a number of reactants which goes on to release light in order to revert to its ground state energy. Chemiluminescence is a simple, low cost and very sensitive technique that has been used for the analysis of compounds in various fields such as clinical and analytical chemistry [15, 16]. Peroxyoxalate chemiluminescence (PO-CL) system is a well-known and powerful method that has been widely utilized in environmental, pharmaceutical and biomedical analyses [1, 17]. PO-CL is based on the reaction between hydrogen peroxide with an activated oxalate that emits clear luminescence light in the presence of different fluorophores [2].

In this paper, we report the synthesis of eosin Yellowish nanoparticles (ESNPs) via the Stöber method and then the

A. Yari (✉) · M. Saidikhah
Department of Chemistry, Faculty of Science, Lorestan University, 68137-17133, Khorramabad, Iran
e-mail: a.yari@ymail.com

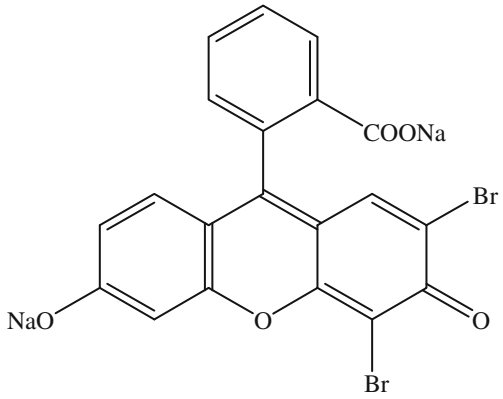

Fig. 1 The chemical structure of 2′,4′,5′,7′-tetrabromo fluorescein disodium salt (Eosin Yellowish, EY)

use of synthesized ESNPs as efficient fluorophores in chemiluminescence reaction of bis(2,4,6-trichlorophenyl) oxalate (TCPO) with hydrogen peroxide in the presence of sodium salicylate (SS).

Experimental

Materials and Apparatus

All chemicals were of analytical grade (from Merck) and used without further purification. TCPO was prepared from the reaction between 2,4,6-trichlorophenol and oxalyl chloride in the presence of triethylamine as described by Mohan and Turro [18]. For PO-CL measurements, freshly prepared solutions were used daily and kept in a dark place.

Transmission electron microscopy (TEM) was performed on a PHILIPS CM120 electron microscope (120 kV) and atomic force microscopy (AFM) analysis was taken using a Dual scope/Raster scope C26-DME microscope. A Shimadzu 1650 (Japan) UV-Vis spectrophotometer was used to record the electronic absorption spectra. The FT-IR spectra were collected on a FT-IR 8400s (Japan) spectrophotometer. The chemiluminescence and fluorescence spectra were recorded on a Perkin-Elmer LS-50 spectrofluorometer.

Synthesis of Eosin Yellowish Doped Silica Nanoparticles

As schematically shown in Fig. 2, the preparation of ESNPs was achieved by the hydrolysis and condensation of TEOS in a mixture of ethanol, water and ammonia. The appropriate amount of EY was dissolved in a mixture of ethanol and ammonia that then dispersed by sonication for 10 min. Then TEOS was added into the vessel dropwise while the mixture being stirred. The stirring was continued for 1 h and the results centrifuged at 8000 rpm for 10 min to obtain the produced NPs. Finally, the NPs were filtered and washed three times with ethanol and distilled water alternatively.

Results and Discussion

Characterization of ESNPs

The Stöber's method includes two basic steps as follows:

$$Si(OC_2H_5)_4 + 4H_2O \xrightarrow{NH_3} Si(OH)_4 + 4C_2H_5OH \quad (1)$$

$$Si(OH)_4 \xrightarrow{H_2O} [SiO_2](OH)_8 \quad (2)$$

At first, TEOS hydrolyzes into silicon tetra hydroxide in the presence of ammonia in ethanol solution while silica nanoparticles are resulted by a poly-condensation reaction in the second step. As has been reported before [9], larger sized NPs could be synthesized by increasing the amount of ammonia.

Here, in order to be encapsulated inside the silica nanoparticles, we added EY at beginning the hydrolysis reaction. The morphology and sizes of the resulted ESNPs were investigated by TEM and AFM measurements. We could synthesis three different sized 300, 400 and 500 nm ESNPs

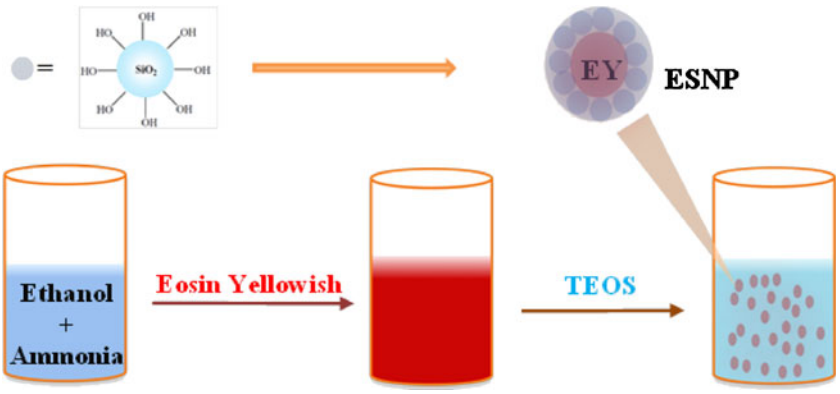

Fig. 2 A schematically presentation of the preparation of ESNPs achieved by hydrolysis and condensation of TEOS in a mixture of ethanol, water and ammonia

by controlling the concentration of ammonia in the solution. The conditions are summarized in Table 1. TEM (Fig. 3) reveals that all NPs demonstrate spherical morphologies with a low aggregation which is due to the interaction between the hydroxyl groups on the surface of NPs. As seen, some of the spherical images show that cores of particles are denser than their outer layers. This fact confirms that the synthesized nanoparticles are including two inner and outer spherical layers, within them the doped dye cores are surrounded by peripheral silica particles, respectively.

Using AFM micrograph of each sample, we studied the dimensions of ESNPs. A typical sample is demonstrated in Fig. 4 (b and c), in which the particle dimensions are clearly measureable (a and d).

Figure 5 presents the FT-IR spectra of EY (a) and ESNPs (b). From this figure, the absorption bands for carboxylic acid stretching (3250–3500 cm^{-1}) are slightly broader for the case EY is encapsulated by NPs because of interaction between this functional group and silanol hydroxyls. The vibration bands of surface silanols are appeared in 960 cm^{-1} while the peak at 797 cm^{-1} can be assigned to the symmetric stretching vibration of Si-O. The peak at 1090 cm^{-1} is due to the asymmetric stretching vibration of the Si-O-Si band. Comparison the fingerprint regions in (a) and (b) show that the structural vibration characteristics of EY have changed extremely when incorporated into NPs that is indicative the encapsulation of this molecule by silica particle.

Figure 6 displays the electronic absorption spectra of EY in the absence (a) and in the presence of NPs (b). The absorption spectra of ESNPs show a maximum around 517 nm, which appear at the absorption region of EY. This reveals that the electronic structure of EY has not been changed at all while the shoulders of the spectra for (b) are at higher levels (relative to the horizontal axis). These facts confirm existence of EY as a core within the produced silica nanoparticles.

As can be seen from the spectra shown in Fig. 7, the fluorescence spectra of free EY is the same as the encapsulated in NPs' cage, which proves the fluorophore was retained without any considerable change in structural characteristics. In addition, the emission light of ESNPs are more intense than free EYs, from which we can say that the fluorophores are protected from the external conversion within a more rigid matrix and prevented from giving up the excitation energies in non-radiative pathways.

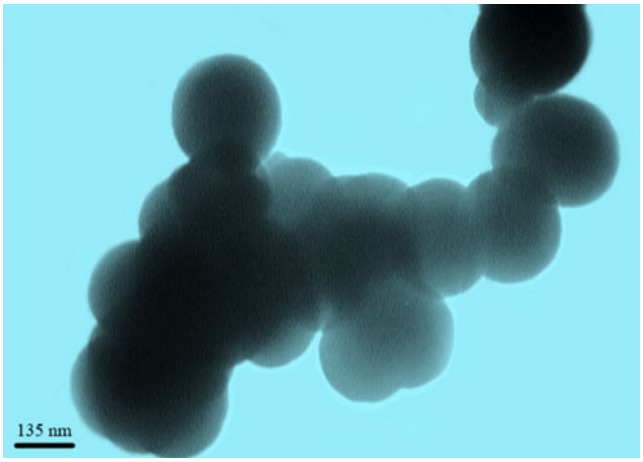

Fig. 3 A TEM image of ESNPs of 300 (±1) nm (the composition of reagents for the synthesized particles is listed in Table 1)

ESNPs as Fluorophores in a Chemiluminescent Reaction

Theoretical Aspects

In 1963 Chandross [19] found a bluish white light from the reaction of oxalyl chloride and hydrogen peroxide in the presence of 9,10-diphenylanthracene. Hydrogen peroxide reacts with aryl oxalate ester to form one or more energy-rich intermediates capable of exciting different types of fluorophores through chemically initiated electron exchange luminescence (CIEEL) mechanism [20]. Fluorophores or fluorescent molecules could be divided into three groups, organic dyes, biological fluorophores and quantum dots [21–26].

As we have already mentioned, DDS has been developed as a new type of fluorophores in recent years. However, to the best of our knowledge, this is the first time that a DDS is applied in a PO-CL system as a fluorophore. The proposed mechanism for PO-CL reaction is shown in Scheme 1. In the first step, an aryl oxalate ester (like TCPO) react with hydrogen peroxide to produce a key intermediate 1,2-dioxetanedione. The decomposition of 1,2-dioxetanedione produces an oxalate biradical intermediate, which releases two carbon dioxide molecules having enough energy to sensitize the fluorophore [27]. Ultimately, the excited fluorophore returns to the ground state and gives up its energy by emission of light.

Table 1 The conditions for synthesis of three different sized ESNPs by controlling the concentration of ammonia in the solution

Eosin yellowish (g)	Ethanol (mL)	NH_4OH (30%) (mL)	TEOS (mL)	Mean diameter (nm)
0.1	11.5	4.5	2.5	300.0 (±1.0)
0.1	9	7	2.5	400.0 (±1.1)
0.1	6	10	2.5	500.0 (±5.2)

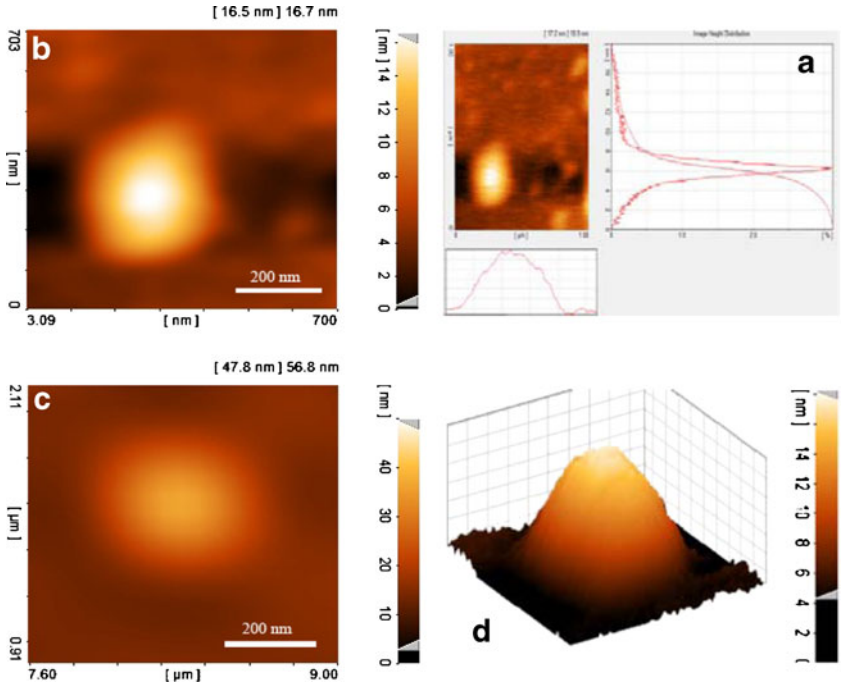

Fig. 4 A typical sample topography from AFM micrograph images of ESNPs with different amounts of reagents (**b** and **c**), from which the particle dimensions are measureable (**a** and **d**)

Experimental Results

The reaction was initiated by injecting 100 μL solution of 2.0 M H_2O_2 (in acetonitrile) to a fluorescence measuring cell containing 1.5 mL of 6.80×10^{-4} g/mL EY or 2.0×10^{-4} g/mL of ESNPs, 100 μL of 5.3×10^{-3} M TCPO (in ethyl acetate) and 100 μL of 2.5×10^{-2} M SS (in methanol) at room temperature. The resulted chemiluminescence

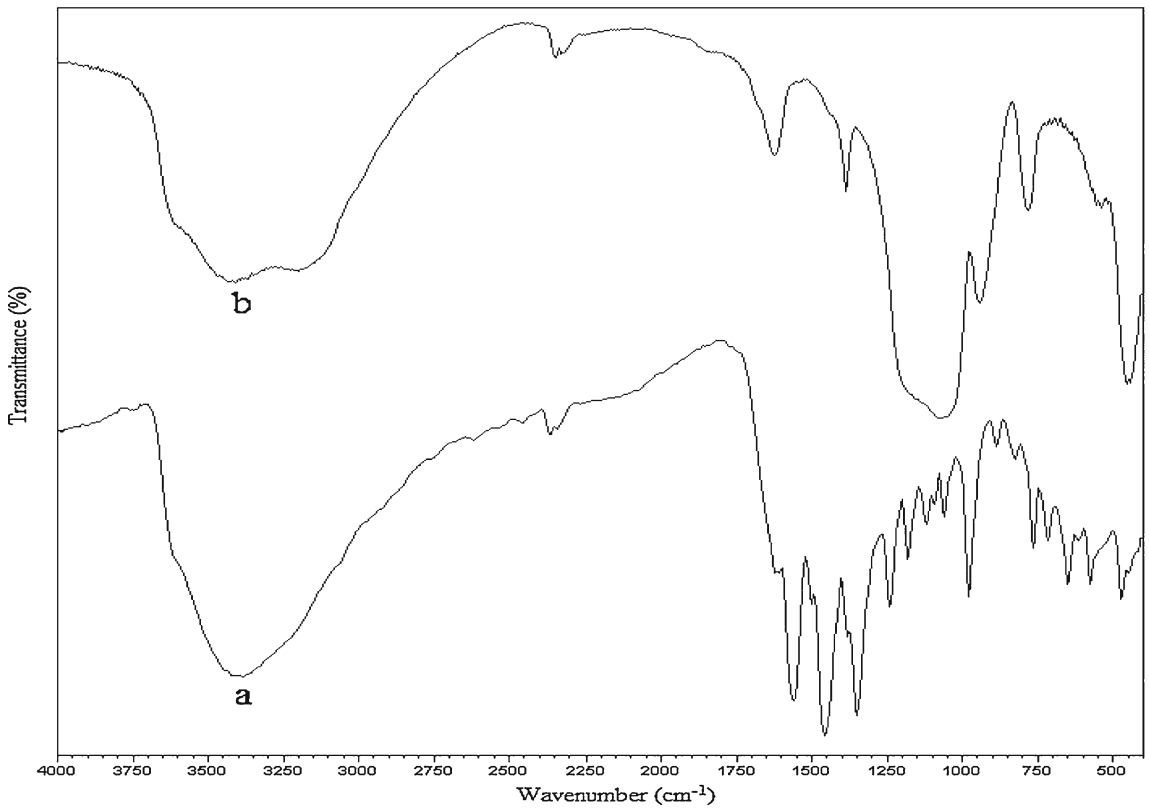

Fig. 5 The FT-IR spectra of EY (**a**) and ESNPs (**b**)

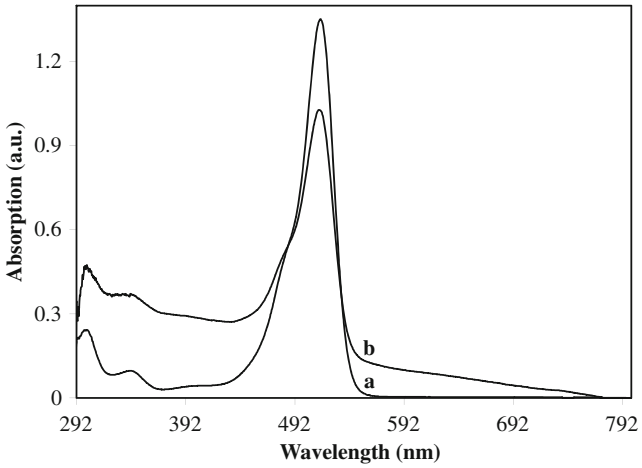

Fig. 6 The electronic absorption spectra of EY (**a**) and ESNPs (**b**). The absorption spectra of ESNPs show a maximum around 517 nm, which appears at the absorption region of EY

spectra are shown in Fig. 8. As demonstrated in this figure, there are no differences between the chemiluminescence spectra of the fluorophores EY (a) and ESNPs (b). This implies that the energy transfer is governed by long-range fashion (Förster resonance energy transfer) [28] and should be named as an indirect chemiluminescence.

The PO-CL reaction of the present system was also studied using a UV-visible spectrophotometric method. In Fig. 9, UV-visible spectra for the chemiluminescence system before (a) and after (b) the PO-CL reaction are shown. This figure illustrates that the spectral characteristics of the absorbing system (EY) have not been changed during the chemiluminescence reaction, at which no decomposition or

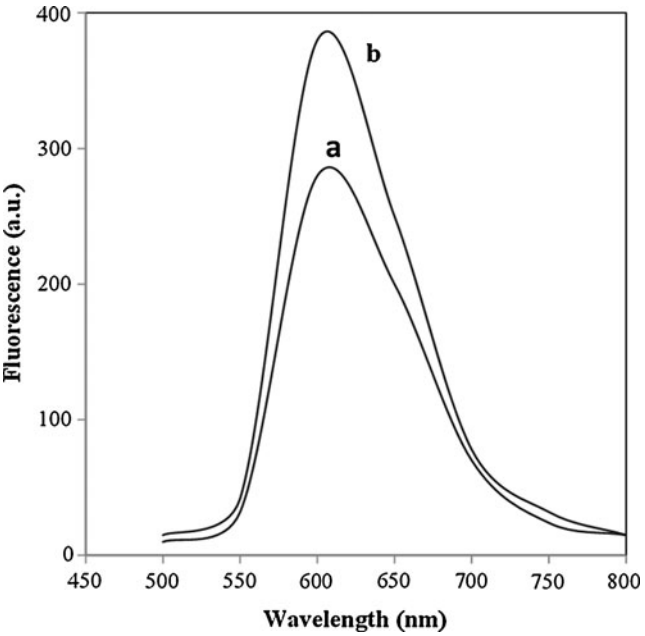

Fig. 7 Fluorescence emission spectra of (**a**) EY and (**b**) ESNPs in ethanol

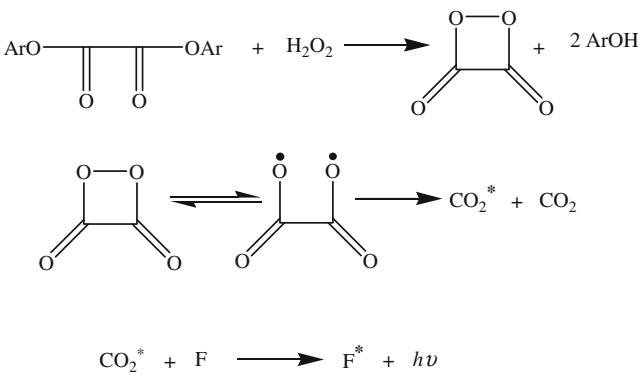

Scheme 1 The proposed mechanism for the PO-CL reaction of DDS

any side reaction has occurred along the energy transfer process. However, the minor decrease in the absorption of the peak at 519 nm could be due to dilution by addition of the required agents for initiation the chemiluminescence reaction.

In order to investigate the influence of sizes of the particles on chemiluminescence signal of the system, the intensity-time plots for three typical particles sizes 300, 400 and 500 nm were constructed and the results are shown in Fig. 10. This figure reveals that the chemiluminescence intensity of the system collapses when the sizes of the particles are increased. This fact is actually in good agreement with the proposed long-range energy transfer mode that governs the luminescence route, in which the larger sized particles have more difficulties to absorb the sensitizing energy because of further distance between the energy donor and acceptor. However, we used the ESNP size of 300.0 (±1.0) nm in subsequent studies.

Optimization of the Required Reagents for the PO-CL System

As expected, the intensity of the PO-CL emission was found to be affected by the type of solvent [29]. Therefore, the role of type of solvent on chemiluminescence emission was studied, for which the influences of different solvents on the PO-CL intensity were examined while the concentrations of all other reactants were kept constant. The results (Fig. 11) indicated that THF enhances chemiluminescence signal intensity more than other used solvents acetone, acetonitrile and ethyl acetate. So, THF was selected as the best solvent for the reaction. However, the chemiluminescence intensities nearly were quenched in dimethyl formamide, dimethyl sulfoxide, ethanol and methanol.

The effects of various concentrations of effective reactants were investigated and the results are demonstrated in Fig. 12. It was found that the signal increases with increasing in the concentration of SS (Fig. 12a) until a concentration of 5.94×10^{-5} M is reached, which confirms the

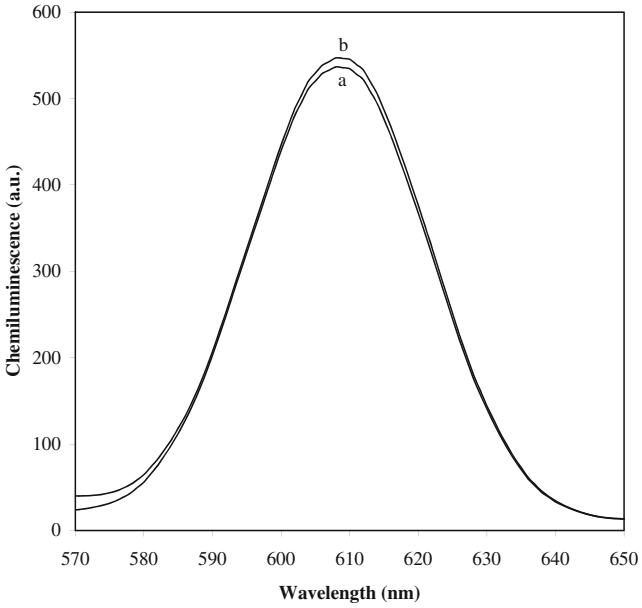

Fig. 8 Chemiluminescence spectra of the fluorophores EY (**a**) and ESNPs (**b**)

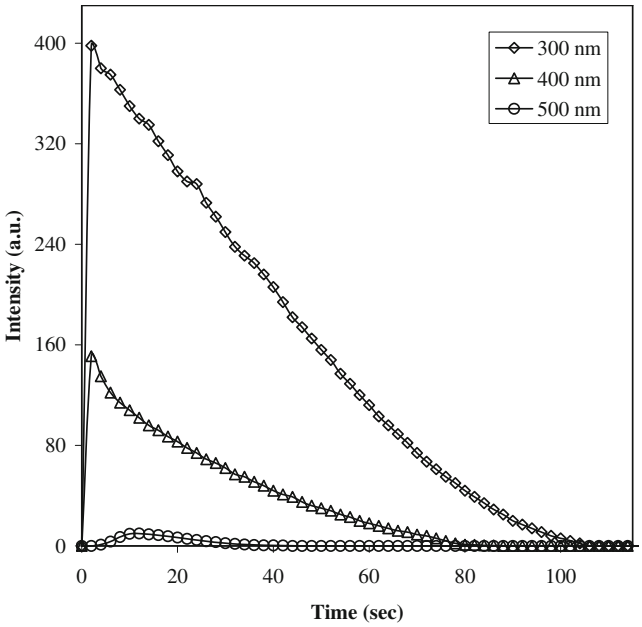

Fig. 10 The effect of particle size on the chemiluminescence of PO-CL system

catalytic role of SS in the PO-CL system [30]. The chemiluminescence intensity was nearly constant in the range 5.94×10^{-5}–9.49×10^{-5} M where the intensities falls extremely at higher concentrations of SS that maybe due to the decomposition of 1,2-dioxetanedione. Thus, the optimum concentration of SS 7.50×10^{-5} M was selected for next investigations.

The chemiluminescence response of the H_2O_2-TCPO-SS-ESNPs system was measured against the concentrations of H_2O_2 (Fig. 12b). The emission intensity sharply increases with increasing the concentration of H_2O_2 until 6.53×10^{-3} M but there was a gradually increase in the emission intensity in the concentration range of 1.39×10^{-2}–3.67×10^{-2} M. However, chemiluminescence intensity was relatively constant in the range of 3.67×10^{-2}–4.57×10^{-2} M of H_2O_2. Thus, we used 4.0×10^{-2} M as optimal concentration for the further studies.

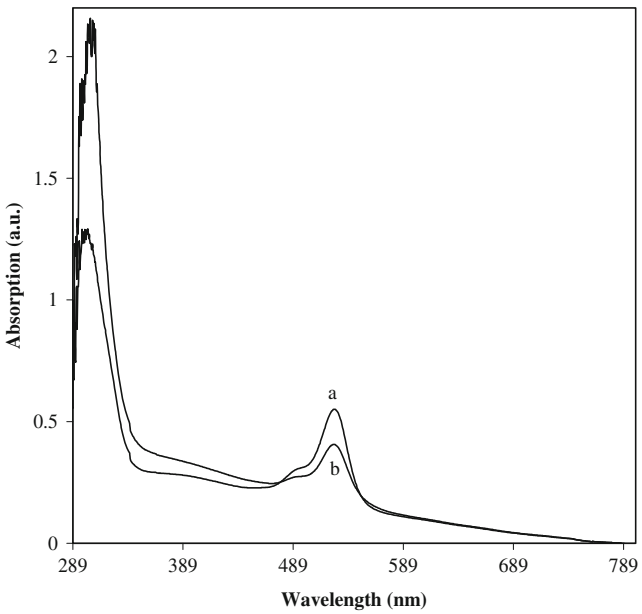

Fig. 9 UV-visible spectra for PO-CL 300 (±1.0) ESNPs (**a**) before and (**b**) after the injection of H_2O_2

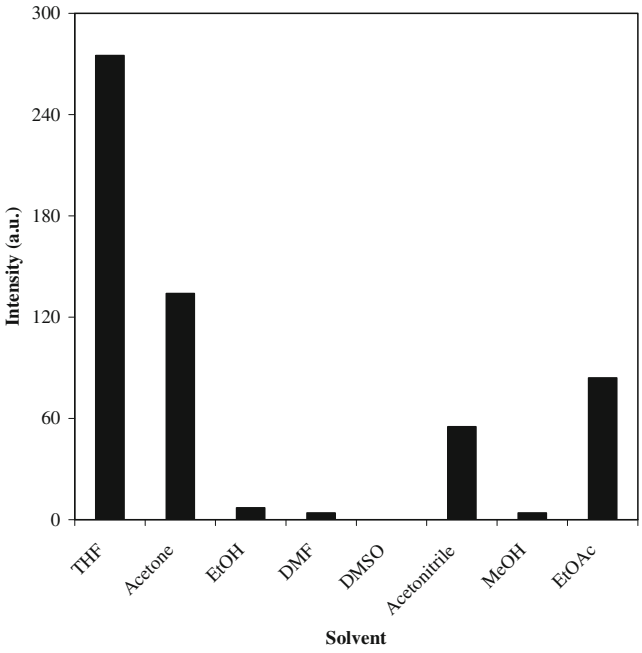

Fig. 11 The influence of the type of solvent on the chemiluminescence emission of the ESNPs:SS:TCPO:H_2O_2 system with concentrations of 6.8×10^{-4} g/mL, 2.5×10^{-2} M, 5.3×10^{-3} M and 1.965 M, respectively

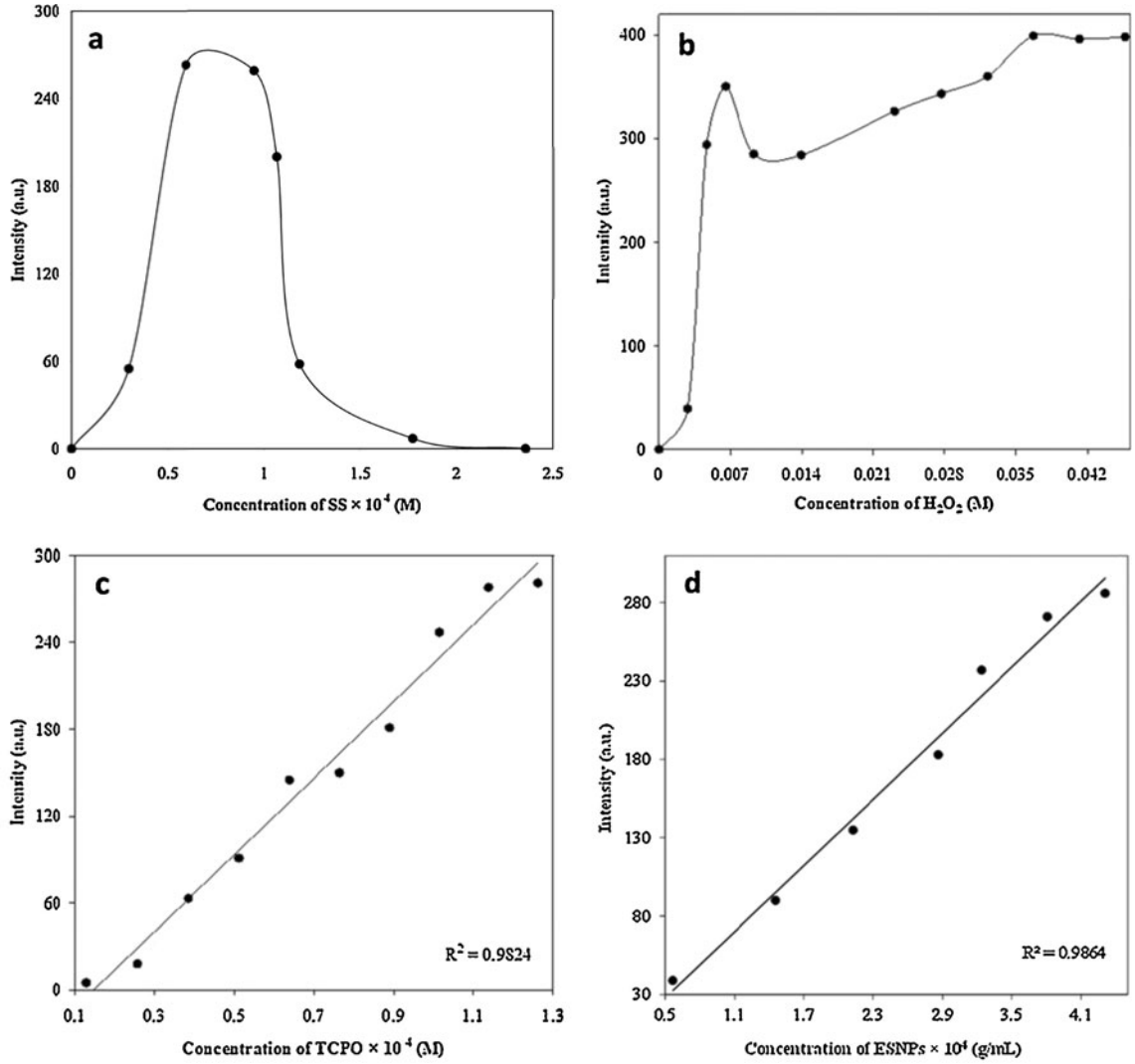

Fig. 12 The effect of concentrations (**a**) of SS (0.00–2.36×10^{-4} M) on the intensity of TCPO (7.50×10^{-5} M), ESNPs (2.12×10^{-4} g/mL) and H_2O_2 (4.00×10^{-2} M) system; (**b**) of H_2O_2 (0.00–4.57×10^{-2} M) in the system containing SS (7.50×10^{-5} M), TCPO (5.12×10^{-5} M) and ESNPs (2.12×10^{-4} g/mL); (**c**) chemiluminescence intensity in the presence of the SS:H_2O_2:ESNPs with concentrations of 7.50×10^{-5} M, 4.00×10^{-2} M and 2.12×10^{-4} g/mL, respectively, over the range of 1.29×10^{-5} to 1.26×10^{-4} M of TCPO; (**d**) The chemiluminescence intensity as a function of ESNPs concentrations (5.67×10^{-5} to 4.31×10^{-4} g/mL) in the presence of SS (7.50×10^{-5} M), H_2O_2 (4.00×10^{-2}) and TCPO (5.12×10^{-5} M) system

The chemiluminescence intensity of the system was studied over the range of 1.29×10^{-5} to 1.26×10^{-4} M of TCPO. The effect of TCPO concentration resulted in construction a plot was linear with r=0.98 (Fig. 12c). These results show that the intensities will increase linearly if we increase the concentration of TCPO in the solution. Therefore, 5.12×10^{-5} M TCPO was chosen as optimal concentration.

Finally, the study of influence of the ESNPs concentration on the intensity of the emitted light showed that there is a linear relationship between the emission intensity and the concentration of ESNPs (Fig. 12d). From this relationship, we used 2.12×10^{-4} g/mL of ESNPs as the best concentration for any emission measurement. Optimum values for different variables are summarized in Table 2.

Evaluation the Activation Parameters

Effect of temperature on intensity of emitted light is a very important factor that an analyst should investigate during the

Table 2 Summary of the optimal conditions were used for the chemiluminescence of EYNPs

Variables	Optimum value
Solvent type	THF
Particle size	300 (±1.0) nm
SS	7.50×10^{-5} M
TCPO	5.12×10^{-5} M
H_2O_2	4.00×10^{-2} M
ESNPs	2.12×10^{-4} g/mL

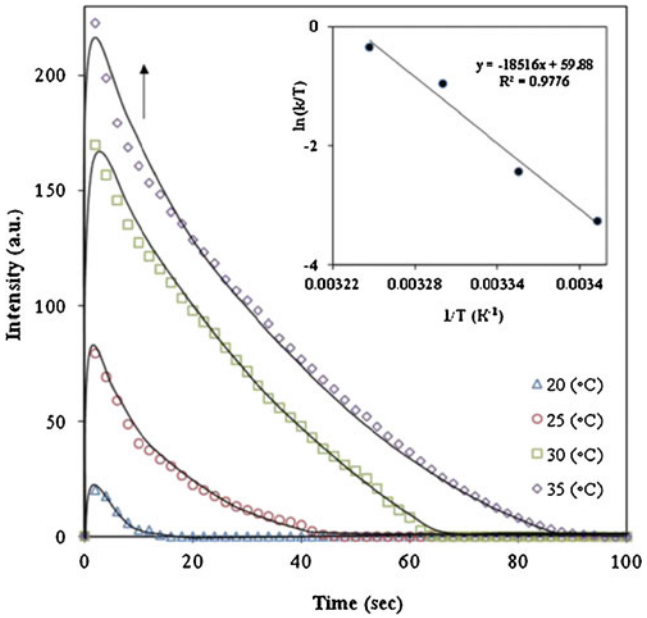

Fig. 13 The chemiluminescence intensity-time plot of ESNPs-TCPO-H_2O_2-SS (2.12×10^{-4} g/mL, 5.12×10^{-5}, 4.00×10^{-2}, 7.50×10^{-5} M) system at different temperatures. The inset shows the plot of ln(k/T) against 1/T, from which the activation parameters are evaluated

study of chemiluminescence of a system. The method for such a study has already been introduced by Eyring's transition-state theory [31, 32]. We will be considering the bimolecular reaction of A with B to form C, as shown below:

$$A + B \xrightarrow{k} C \tag{3}$$

k is the bimolecular rate constant for conversion of A and B to C. According to the transition state model, the reactants are getting over into an unsteady intermediate state (AB^*) on the reaction pathway:

$$A + B \underset{k_r}{\overset{k_f}{\leftrightarrow}} AB^* \xrightarrow{k^*} C \tag{4}$$

In this equation, k^* is the unimolecular rate constant for decomposition of the activated complex AB^* to form C, k_f and k_r are rate constants for the forward and the backward reactions, respectively. The high-energy complex represents an unstable molecular arrangement, in which bonds break and form to generate the product C or to degenerate back to the reactants A and B. The linear form of Eyring's equation is finally found as follows:

$$\ln\left(\frac{k}{T}\right) = -\frac{\Delta H^*}{R}\cdot\frac{1}{T} + \ln\left(\frac{k_B}{h}\right) + \frac{\Delta S^*}{R} \tag{5}$$

$k = k^*.k_B.T/h$, where k_B is Boltzmann constant (1.381×10^{-23} $J.K^{-1}$), h is Palnk constant (6.626×10^{-34} J.s), ΔH^* and ΔS^* are activation enthalpy and entropy changes, respectively. T is absolute temperature (in degrees Kelvin) and R is universal gas constant (8.3144 $J.mol^{-1}.K^{-1}$). Clearly, a plot of ln(k/T) versus 1/T produces a straight line that ΔH^* can be calculated from the slope of this line. A precise determination of the activation enthalpy (and the other activation parameters) requires at least three different rate constants. This means three kinetic runs at different temperatures should be carried out.

The influences of different temperatures of the reaction solution 293, 298, 303 and 308 K on the chemiluminescence of the system were studied under the optimized condition (Fig. 13, points). This figure shows that the intensity of the system increases when the temperature of the solution rises. From Eyring's transition-state theory, the corresponding response curves were constructed theoretically (Fig. 13, solid lines) by using the computerized curve-fitting program KINFIT [33]. As shown in this figure, the experimental data fits the theoretically predicted values very good that is indicative the proposed rate mechanism steps are governed by a bimolecular fashion. The theoretically predicted activation parameters thus were determined as listed in Table 3.

In addition, using the plot of ln(k/T) versus 1/T, the activation parameters ΔH^* and ΔS^* of the system were evaluated from the slope and intercept of the linear regression plot of ln(k/T) versus 1/T (inset in Fig. 13). Gibb's free energy change (ΔG^*) and activation energy (E_a) were also evaluated. Thus, they were determined as follows: $\Delta H^*\left(153.94\,\mathrm{kJ\,mol^{-1}}\right)$, $\Delta S^*\left(3.30\,\mathrm{kJ\,mol^{-1}\,K^{-1}}\right)$, $\Delta G* = 153.94 - 3.30T(r = 0.997)$ and $E_a = 153.94 + 0.008T\,(r = 0.999)$.

As seen, a positive value for entropy of activation indicates that the transition state is highly disordered compared to the ground state. Degrees of freedom are

Table 3 Activation parameters evaluated from the temperature-effect study

Temperatures (K)	k (s^{-1})	ΔH* (kJ mol^{-1})	ΔS* (kJ mol^{-1} K^{-1})	−ΔG* (kJ mol^{-1})
293	217.3±5.2	17.4±0.7	3.4±0.1	1029.9±6.7
298	115.7±3.8	19.3±0.8	2.7±0.1	798.8±4.1
303	25.9±1.4	22.2±1.1	1.5±0.1	424.9±2.8
308	11.1±0.2	30.1±1.3	1.1±0.1	292.0±1.6

'liberated' in going from the ground state to the transition state, which, in turn, increase the rate of the reaction. The existence of a bimolecular interaction between the intermediate 1,2-dioxetanedione (C_2O_4) and ESNPs, which is in agreement with the CIEEL mechanism in the chemi-excitation step and excludes the ESNPs excitation by an electronic energy transfer [7], proves the proposed theoretical models.

As shown in Fig. 13, a clear increase in chemiluminescence signal is observed at higher temperature which is probably due to the increase in the population of excited ESNPs at higher temperatures that proves the enhanced chemiluminescence intensity at higher temperatures due to the higher rate constants [34].

Conclusion

In this work, we have synthesized a new dye-doped (DDS) fluorophore by using the Stöber method. The synthesized Eosin yellowish silica nanoparticles showed excellent stability. Based on the obtained results, it can be inferred that such optimized core/shell architectures could be expanded to be a unique platform for potential applications such as the detection of analytes formed during in situ chemical transformations. Here, this is the first time that a DDS is applied in a PO-CL system as a fluorophore. We created highly sensitive particles capable of being used as fluorophore in a PO-CL system that emits an intense light, thus leading to monitor analytes in real samples.

References

1. Dodeigne C, Thunus L, Lejeune R (2000) Chemiluminescence as diagnostic tool, a review. Talanta 51:415–439
2. Wada M, Abe K, Ideka R, Harada S, Kuroda N, Nakashima K (2010) Enhancement of peroxyoxalate chemiluminescence intensity by surfactants and its application to detect detergent. Talanta 81:1133–1136
3. Chen X, Zhao T, Zou J (2009) A novel mimetic peroxidase catalyst by using magnetite-containing silica nanoparticles as carriers. Microchim Acta 164:93–99
4. Yao G, Wang L, Wu Y, Smith J, Xu J, Zhao W, Lee E, Tan W (2006) FloDots: luminescent nanoparticles. Anal Bioanal Chem 385:518–524
5. Gao F, Chen X, Ye Q, Yao Z, Guo X, Wang L (2011) Core-shell fluorescent silica nanoparticles for sensing near-neutral pH values. Microchim Acta 172:327–333
6. Koole R, Schooneveld MMV, Hilhorst J, Castermans K, Cormode DP, Strijkers GJ, Donega CDM, Vanmaekelbergh D, Griffioen AW, Nicolay K, Fayad ZA, Meijerink A, Mulder WJM (2008) Paramagnetic lipid-coated silica nanoparticles with a fluorescent quantum dot core: a new contrast agent platform for multimodality imaging. Bioconjugate Chem 19:2471–2479
7. Xu Y, Li Q (2007) Multiple fluorescent labeling of silica nanoparticles with lanthanide chelates for highly sensitive time-resolved immunofluorometric assays. Clin Chem 53:1503–1510
8. Knopp D, Tang D, Niessner R (2009) Review: bioanalytical applications of biomolecule-functionalized nanometer-sized doped silica particles. Anal Chim Acta 647:14–30
9. Stöber W, Fink A, Bohn E (1986) Controlled growth of monodisperse silica spheres in the micron size range. J Colloid Interface Sci 26:62–69
10. Song X, Li F, Ma J, Jia N, Xu J, Shen H (2011) Synthesis of fluorescent silica nanoparticles and their applications as fluorescence probes. J Fluoresc 21:1205–1212
11. Canton G, Ricco R, Marinello F, Carmignato S, Enrichi F (2011) Modified Stöber synthesis of highly luminescent dye-doped silica nanoparticles. J Nanopart Res 13:4349–4356
12. Hazebroucq S, Labat F, Lincot D, Adamo C (2008) Theoretical insights on the electronic properties of Eosin Y, an organic dye for photovoltaic applications. J Phys Chem 112:7264–7270
13. Hadjmohammadi MR, Chaichi MJ, Yousefpour M (2008) Solvatochromism effect of different solvents on UV-Vis spectra of fluorescein and its derivatives. Iran J Chem Chem Eng 27:9–14
14. Shen Y, Nonomura K, Schlettwein D, Zhao C, Wittstock G (2006) Photoelectrochemical kinetics of Eosin Y-sensitized zinc oxide films investigated by scanning electrochemical microscopy. Chem Eur J 12:5832–5839
15. Kricka LJ (2003) Clinical applications of chemiluminescence. Anal Chim Acta 500:279–286
16. Liu M, Lin Z, Lin JM (2010) A review on applications of chemiluminescence detection in food analysis. Anal Chim Acta 6(70):1–10
17. Tsunoda M, Imai K (2005) Analytical applications of peroxyoxalate chemiluminescence. Anal Chim Acta 541:13–23
18. Mohan AG, Turro NJ (1974) A facile and effective chemiluminescence demonstration experiment. J Chem Educ 51:528–529
19. Chandross EA (1963) A new chemiluminescent system. Tetrahedron Lett 12:761–765
20. Schuster GB (1979) Chemiluminescence of organic peroxides. Conversion of ground-state reactants to excited-state products by the chemically initiated electron-exchange luminescence mechanism. Accounts Chem Res 12:366–373
21. Ahmed S, Kishikawa N, Ohyamam K, Wada M, Nakashimam K, Kuroda N (2009) Selective determination of doxorubicin and doxorubicinol in rat plasma by HPLC with photosensitization reaction followed by chemiluminescence detection. Talanta 78:94–100
22. Ferrari BC, Bergquist PL (2007) Quantum dots as alternatives to organic fluorophores for cryptosporidium detection using conventional flow cytometry and specific monoclonal antibodies: lessons learned. Cytometry 71:265–271
23. Tsein RY (1998) The green fluorescent protein. Annu Rev Biochem 67:509–544
24. Melnik TN, Povarnitsyna TV, Glukhov AS, Uversky VN, Melnik BS (2011) Sequential melting of two hydrophobic clusters within the green fluorescent protein GFP-cycle3. Biochem 50:7735–7744
25. Frasco MF, Chaniotakis N (2009) Semiconductor quantum dots in chemical sensors and biosensors. Sensors 9:7266–7286
26. Peral RI, Bergquist PL, Walter MR, Gibbs M, Goldys EM, Ferrari B (2008) Potential use of quantum dots in flow cytometry. Int J Mol Sci 9:2622–2638
27. Bos R, Tonkin SA, Hanson GR, Hinson CM, Lim KF, Barnett NW (2009) In search of a chemiluminescence 1,4-dioxy biradical. J Am Chem Soc 131:2770–2771
28. Andrews DL (1989) A unified theory of radiative and radiationless molecular energy transfer. Chem Phys 135:195–201
29. Weinberger R (1984) Solvent and pH effects on peroxyoxalate chemiluminescence detection for liquid chromatography. J Chromatogr 314:155–165
30. Zargoosh K, Chaichi MJ, Asghari S, Qandalee M, Shamsipur M (2010) A study of chemiluminescence from reaction of bis

(2,4,6-trichlorophenyl)oxalate, hydrogen peroxide and diethyl-2-(cyclohexylamino)-5-[(E)-2-phenyl-1-ethenyl]-3,4-furandicarboxylate as a novel fluorescer. J Iran Chem Soc 7:376–383
31. Hadd AG, Robinson AL, Rowlen KL, Birks JW (1998) Stopped-flow kinetics investigation of the imidazole-catalyzed peroxyoxalate chemiluminescence reaction. J Org Chem 63:3023–3031
32. Laidler KJ, King MC (1983) The development of transition-state theory. J Phys Chem 87:2657–2664
33. Dye JL, Nicely VA (1971) A general purpose curve-fitting program for class and research use. J Chem Educ 48:443–450
34. Winzor DJ, Jackson CM (2006) Interpretation of the temperature dependence of equilibrium and rate constants. J Mol Recogn 19:389–407